

# “SINGLE RING THEOREM” AND THE DISK-ANNULUS PHASE TRANSITION

Joshua Feinberg<sup>a\*</sup>, R. Scalettar<sup>b\*</sup> & A. Zee<sup>c\*</sup>

<sup>a)</sup>Physics Department,

University of Haifa at Oranim, Tivon 36006, Israel\*\*

and

Physics Department,

Technion, Israel Institute of Technology, Haifa 32000, Israel

<sup>b)</sup>Physics Department,

University of California, Davis, CA 95616, USA

<sup>c)</sup>Institute for Theoretical Physics

University of California

Santa Barbara, CA 93106, USA

## Abstract

Recently, an analytic method was developed to study in the large  $N$  limit non-hermitean random matrices that are drawn from a large class of circularly symmetric non-Gaussian probability distributions, thus extending the existing Gaussian non-hermitean literature. One obtains an explicit algebraic equation for the integrated density of eigenvalues from which the Green's function and averaged density of eigenvalues could be calculated in a simple manner. Thus, that formalism may be thought of as the non-hermitean analog of the method due to Brézin, Itzykson, Parisi and Zuber for analyzing hermitean non-Gaussian random matrices. A somewhat surprising result is the so called “Single Ring” theorem, namely, that the domain of the eigenvalue distribution in the complex plane is either a disk or an annulus. In this paper we extend previous results and provide simple new explicit expressions for the radii of the eigenvalue distribution and for the value of the eigenvalue density at the edges of the eigenvalue distribution of the non-hermitean matrix in terms of moments of the eigenvalue distribution of the associated hermitean matrix. We then present several numerical verifications of the previously obtained analytic results for the quartic ensemble and its phase transition from a disk shaped eigenvalue distribution to an annular distribution. Finally, we demonstrate numerically the “Single Ring” theorem for the sextic potential, namely, the potential of lowest degree for which the “Single Ring” theorem has non-trivial consequences.

---

\**e-mail addresses:* [joshua@physics.technion.ac.il](mailto:joshua@physics.technion.ac.il), [rst@solid.ucdavis.edu](mailto:rst@solid.ucdavis.edu), [zee@itp.ucsb.edu](mailto:zee@itp.ucsb.edu)

\*\**permanent address*

# 1 Introduction

There has been considerable interest in random non-hermitean matrices in recent years. Possible applications range over several areas of physics[1, 2, 3, 4]. For some recent reviews see[5]. One difficulty is that the eigenvalues of non-hermitean matrices invade the complex plane, and consequently, various methods developed over the years to deal with random hermitean matrices are no longer applicable, as these methods typically all involve exploiting the powerful constraints of analytic function theory. (See in particular the paper by Brézin, Itzykson, Parisi, and Zuber [6].) In [3], two of us proposed a “method of hermitization”, whereby a problem involving random non-hermitean matrices can be reduced to a problem involving random hermitean matrices, to which various standard methods (such as the diagrammatic method[7], or the “renormalization group” method[8, 9, 10, 11]) can be applied. An idea similar to the “method of hermitization” was expressed independently in [2].

To our knowledge, the literature on random non-hermitean matrices[1, 2] has focussed exclusively on Gaussian randomness. For instance, it has been known for over thirty years, from the work of Ginibre[12], that for the Gaussian probability distribution  $P(\phi) = (1/Z)\exp(-N\text{tr}\phi^\dagger\phi)$  (here, as in the rest of this paper,  $\phi$  denotes an  $N \times N$  complex random matrix with the limit  $N \rightarrow \infty$  understood), the density of eigenvalues of  $\phi$  is uniformly distributed over a disk of radius 1 in the complex plane.

Analytic determination of the density of eigenvalues of a non-Gaussian probability distribution of the form

$$P(\phi) = \frac{1}{Z}e^{-N\text{tr}V(\phi^\dagger\phi)}, \quad (1.1)$$

where  $V$  is an arbitrary polynomial of its argument, was given for the first time in [4]. Based on the method of hermitization, it was shown in [4] that by a simple trick, the desired density of eigenvalues could be obtained with a minimal amount of work, by judiciously exploiting the existing literature on random hermitean matrices.

Due to the symmetry of  $P(\phi)$  under the transformation  $\phi \rightarrow e^{i\alpha}\phi$ , the density of eigenvalues is obviously rotational invariant. It was shown in [4] that the class of

probability distributions of the form (1.1) exhibits a universal behavior in the sense that whatever the polynomial  $V$  was, the shape of the eigenvalue distribution in the complex plane was always either a disk or an annulus. This result was referred to in [4] as the “Single Ring Theorem”.

In a certain sense, the formalism developed in [4] may be thought of as the analog of the work of Brézin et al. for random hermitean matrices [6]; they showed how the density of eigenvalues of hermitean matrices  $\varphi$  taken from the probability distribution  $P(\varphi) = (1/Z)\exp[-N\text{tr}V(\varphi)]$  with  $V$  an arbitrary polynomial can be determined, and not just for the Gaussian case studied by Wigner and others[13], in which  $V = (1/2)\text{tr}\varphi^2$ . An important simplifying feature of the analysis in [6] is that  $P(\varphi)$  depends only on the eigenvalues of  $\varphi$ , and not on the unitary matrix that diagonalizes it. In contrast, the probability distribution (1.1) for non-hermitean matrices depends explicitly on the  $GL(N)$  matrix  $S$  used to diagonalize  $\phi = S^{-1}\Lambda S$ , and  $S$  does not decouple. Remarkably however, for the Gaussian  $P(\phi)$ , Ginibre [12] managed to integrate over  $S$  explicitly and derived an explicit expression for the probability distribution of the eigenvalues of  $\phi$ . Unfortunately, it is not clear how to integrate over  $S$  and derive the expression for the eigenvalue probability distribution for non-Gaussian distributions of the form (1.1). In [4] this difficulty was circumvented by using the method of hermitization.

As an explicit example, the case  $V(\phi^\dagger\phi) = 2m^2\phi^\dagger\phi + g(\phi^\dagger\phi)^2$  was studied in detail in [4]. As should perhaps be expected in advance, the following behavior in the parameter space  $m^2, g > 0$  was found: for  $m^2$  positive, the eigenvalue distribution was disk-like (and non-uniform), generalizing Ginibre’s work, but as  $m^2 \equiv -\mu^2$  was made more and more negative, a phase transition at the critical value

$$\mu_c^2 = \sqrt{2g}$$

occured, after which the disk fragmented into an annulus. The density of eigenvalues was calculated in [4] in detail.

The paper is organized as follows: In Section 2 we summarize the “method of hermitization” [3]. We present (without derivation) the general algorithm for finding

the density of eigenvalues associated with (1.1) which was developed in [4], and also add some new insight into the mechanism behind the “Single Ring” theorem. We then formulate a novel simple criterion on the couplings in  $V(\phi^\dagger\phi)$  to decide whether the shape of the eigenvalue distribution is a disk or an annulus. Finally, we discuss some generic features of the disk-annulus phase transition. In particular, we prove that the Green’s function associated with the hermitean matrix  $\phi^\dagger\phi$  (which plays an important role in the “hermitization algorithm” just mentioned) is continuous through the disk-annulus phase transition.

In Section 3 we provide simple new expressions for the outer radius  $R_{out}$  and for the inner radius  $R_{in}$  (in the annular phase) of the eigenvalue distribution of the non-hermitean matrix  $\phi$ , and for the corresponding boundary values  $\rho(R_{out})$  and  $\rho(R_{in})$  of its eigenvalue density, in terms of the moments

$$\langle \sigma^k \rangle = \int d\sigma \sigma^k \tilde{\rho}(\sigma) \quad (k = 0, \pm 1, \dots)$$

of the eigenvalue distribution  $\tilde{\rho}(\sigma)$  of the hermitean matrix  $\phi^\dagger\phi$ . Thus, we find that

$$R_{out}^2 = \langle \sigma \rangle$$

and

$$\rho(R_{out}) = \frac{2R_{out}^2}{\langle \sigma^2 \rangle - \langle \sigma \rangle^2}.$$

We see that  $R_{out}^2$  is simply the average of  $\sigma$ , and the density  $\rho(R_{out})$  is inversely proportional to the variance of  $\sigma$ .

Similarly, we find that in the annular phase,

$$\frac{1}{R_{in}^2} = \left\langle \frac{1}{\sigma} \right\rangle$$

and

$$\rho(R_{in}) = \frac{2R_{in}^{-6}}{\langle \sigma^{-2} \rangle - \langle \sigma^{-1} \rangle^2}.$$

Thus,  $R_{in}^{-2}$  is simply the  $\sigma^{-1}$  moment of  $\tilde{\rho}(\sigma)$ , and the density  $\rho(R_{out})$  is inversely proportional to the variance of  $\sigma^{-1}$ .

In Section 4 we verify that the explicit analytic expressions in [4] concerning the quartic ensemble  $V(\phi^\dagger\phi) = 2m^2\phi^\dagger\phi + g(\phi^\dagger\phi)^2$  are consistent with the results of Section 3. We also compare these analytic predictions with results of Monte-Carlo simulations of the quartic ensemble for various values of  $m^2$  and  $g$ . The numerical results we obtained for the eigenvalue distribution in the disk phase and in the annular phase, as well as some quantitative features of the disk-annulus transition are in good agreement with the analytic predictions in [4].

The “Single Ring Theorem” may seem surprising at first sight. Our explanation of why the single ring theorem is not that surprising rests upon the simple argument that fragmentation of the eigenvalue distribution of  $\phi^\dagger\phi$  into several disjoint segments does not necessarily imply that the eigenvalues of  $\phi$  trace out annuli obtained, loosely speaking, by revolving the segments of the eigenvalue distribution of  $\phi^\dagger\phi$  into the complex plane (see the discussion in Section 2). In Section 5 we carry a numerical check of the “Single Ring” theorem for the sextic potential  $V(\phi^\dagger\phi) = m^2\phi^\dagger\phi + \frac{\lambda}{2}(\phi^\dagger\phi)^2 + \frac{g}{3}(\phi^\dagger\phi)^3$ , which is the potential of lowest degree for which the eigenvalues of  $\phi^\dagger\phi$  may split into more than a single segment (in this case, two segments at the most). We generated numerically an ensemble in which the spectrum of  $\phi^\dagger\phi$  is split into two separated segments, yet we found that the spectrum of  $\phi$  is a disk, and not a configuration of a disk encircled by a concentric annulus, as one would perhaps naively expect by rotating the two-segment spectrum of  $\phi^\dagger\phi$  in the complex plane.

In the Appendix we briefly review the multi-cut phase structure of matrix ensembles with generic  $V(\phi^\dagger\phi)$ , and then specialize to the phase structure of the sextic potential ensemble.

## 2 The Method of Hermitization and Non-Gaussian Ensembles

Here we very briefly summarize the “method of hermitization” [3, 4] in the form of an algorithm, followed by a general discussion of the phase structure of the eigenvalue distribution.

Let us first introduce some notations and definitions. The averaged density of eigenvalues

$$\rho(x, y) = \left\langle \frac{1}{N} \sum_i \delta(x - \operatorname{Re} \lambda_i) \delta(y - \operatorname{Im} \lambda_i) \right\rangle \quad (2.1)$$

of the non-hermitean matrix  $\phi$ , may be determined from the the Green’s function associated with  $\phi$ , namely

$$G(z, z^*) = \left\langle \frac{1}{N} \operatorname{tr} \frac{1}{z - \phi} \right\rangle = \int d^2 x' \frac{\rho(x', y')}{z - z'}, \quad (2.2)$$

in terms of which<sup>1</sup>

$$\rho(x, y) = \frac{1}{\pi} \partial^* G(z, z^*). \quad (2.3)$$

The probability distributions (1.1) studied in this paper are invariant under  $\phi \rightarrow e^{i\alpha} \phi$ , rendering

$$\rho(x, y) \equiv \rho(r)/2\pi \quad (2.4)$$

circularly invariant. Rotational invariance thus leads to a simpler form of the defining formula (2.2) for  $G(z, z^*)$  which reads

$$\gamma(r) \equiv zG(z, z^*) = \int_0^r r' dr' \rho(r'), \quad (2.5)$$

whence

$$\rho(r) = \frac{1}{r} \frac{d\gamma}{dr}. \quad (2.6)$$

---

<sup>1</sup>We use the following notational conventions: for  $z = x + iy$  we define  $\partial \equiv \frac{\partial}{\partial z} = \frac{1}{2} \left( \frac{\partial}{\partial x} - i \frac{\partial}{\partial y} \right)$  so that  $\partial z = 1$ . Similarly, we define  $\partial^* \equiv \frac{\partial}{\partial z^*} = \frac{1}{2} \left( \frac{\partial}{\partial x} + i \frac{\partial}{\partial y} \right)$ , so that  $\partial^* z^* = 1$  and also  $\partial^*(1/z) = \pi \delta^{(2)}(z)$ . Finally, we denote  $|z| = r$ .

Clearly, the quantity  $\gamma(r)$ , which can be thought of as the integrated eigenvalue density, is a positive monotonically increasing function, which satisfies the obvious “sum-rules”

$$\gamma(0) = 0 \quad \text{and} \quad \gamma(\infty) = 1. \quad (2.7)$$

In particular, observe that the first condition in (2.7) insures that no  $\delta(x)\delta(y)$  spike arises in  $\rho(x, y)$  when calculating it from (2.3) with  $G(z, z^*)$  given by (2.5), as it should be.

It was shown in [4] that by applying a simple trick, the desired Green’s function of a non-hermitean random matrix  $\phi$  could be obtained with a minimal amount of work, by judiciously exploiting the existing literature on random hermitean matrices. The algorithm, according to [4], for finding the Green’s function and the averaged eigenvalue density of a non-hermitean random matrix  $\phi$  drawn from a non-Gaussian ensemble  $P(\phi) = (1/Z)e^{-N\text{tr}V(\phi^\dagger\phi)}$  (Eq. (1.1)) is as follows:

Start with the Green’s function<sup>2</sup>

$$F(w) = \left\langle \frac{1}{N} \text{tr}_{(N)} \frac{1}{w - \phi^\dagger\phi} \right\rangle \equiv \int_0^\infty \frac{\tilde{\rho}(\sigma) d\sigma}{w - \sigma}, \quad (2.8)$$

where

$$\tilde{\rho}(\mu) = \frac{1}{N} \langle \text{tr}_{(N)} \delta(\mu - \phi^\dagger\phi) \rangle \quad (2.9)$$

is the averaged eigenvalue density of  $\phi^\dagger\phi$ . Then, the desired equation for  $\gamma(r) \equiv zG(z, z^*)$  is

$$\gamma \left[ r^2 F \left( \frac{\gamma r^2}{\gamma - 1} \right) - \gamma + 1 \right] = 0. \quad (2.10)$$

Thus, given  $F$  one can solve for  $\gamma(r)$  using this master equation.

Eq.(2.10) is an algebraic equation for  $\gamma(r)$  and thus may have several  $r$  dependent solutions. In constructing the actual  $\gamma(r)$  one may have to match these solutions smoothly into a single function which increases monotonically from  $\gamma(0) = 0$  to

---

<sup>2</sup>Of course,  $F(w)$  is already known in the literature on chiral and rectangular block random hermitean matrices for the Gaussian distribution[11, 15, 16, 17], as well as for non-Gaussian probability distributions of the form (1.1) with an arbitrary polynomial potential  $V(\phi^\dagger\phi)$ [18, 19, 20].

$\gamma(\infty) = 1$ . An explicit non-trivial example of such a procedure is the construction of  $\gamma(r)$  in the disk phase of the quartic ensemble[4].

A remarkable property of (2.10) is that it has only two  $r$ -independent solutions:  $\gamma = 0$  and  $\gamma = 1$  [4]. Since the actual  $\gamma(r)$  increases monotonically from  $\gamma(0) = 0$  to  $\gamma(\infty) = 1$ , we immediately conclude from this observation that there can be no more than a single void in the eigenvalue distribution. Thus, in the class of models governed by  $P(\phi) = \frac{1}{Z}e^{-N\text{tr}V(\phi^\dagger\phi)}$  (Eq. (1.1)), the shape of the eigenvalue distribution is either a disk or an annulus, whatever polynomial the potential  $V(\phi^\dagger\phi)$  is. This result is the “Single Ring Theorem” of [4].

The “Single Ring Theorem” may appear counter-intuitive at first sight. Indeed, consider a potential  $V(\phi^\dagger\phi)$  with several wells or minima. For deep enough wells, we expect the eigenvalues of  $\phi^\dagger\phi$  to “fall into the wells”. Thus, one might suppose that the eigenvalue distribution of  $\phi$  to be bounded by a set of concentric circles of radii  $0 \leq r_1 < r_2 < \dots < r_{n_{\max}}$ , separating annular regions on which  $\rho(r) > 0$  from voids (annuli in which  $\rho(r) = 0$ .) A priori, it is natural to assume that the maximal number of such circular boundaries should grow with the degree of  $V$ , because  $V$  may then have many deep minima. Remarkably, however, according to the “Single Ring Theorem” the number of these boundaries is two at the most.

To reconcile this conclusion with the a priori expectation just mentioned, note that while the eigenvalues of the hermitean matrix  $\phi^\dagger\phi$  may split into several disjoint segments along the positive real axis, this does not necessarily constrain the eigenvalues of  $\phi$  itself to condense into annuli. Indeed, the hermitean matrix  $\phi^\dagger\phi$  can always be diagonalized  $\phi^\dagger\phi = U^\dagger\Lambda^2U$  by a unitary matrix  $U$ , with  $\Lambda^2 = \text{diag}(\lambda_1^2, \lambda_2^2, \dots, \lambda_N^2)$ , where the  $\lambda_i$  are all real. This implies that  $\phi = V^\dagger\Lambda U$ , with  $V$  a unitary matrix as well. Thus, the complex eigenvalues of  $\phi$  are given by the roots of  $\det(z - \Lambda W) = 0$ , with  $W = UV^\dagger$ . Evidently, as  $W$  ranges over  $U(N)$  (which is what we expect to happen in the generic case), the eigenvalues of  $\Lambda W$  could be smeared (in the sense that they would not span narrow annuli around the circles  $|z| = |\lambda_i|$ .)

The last argument in favor of the “Single Ring Theorem” clearly breaks down

when  $W$  fails to range over  $U(N)$ , which occurs when the unitary matrices  $U$  and  $V$  are correlated. For example,  $\phi$  may be such that  $W = UV^\dagger$  is block diagonal, with the upper diagonal block being a  $K \times K$  unitary diagonal matrix  $\text{diag}(e^{i\omega_1}, \dots, e^{i\omega_K})$  (and with  $K$  a finite fraction of  $N$ ). In the extreme case  $K = N$ , in which  $W$  is completely diagonal,  $W \equiv e^{i\omega} = \text{diag}(e^{i\omega_1}, \dots, e^{i\omega_N})$ , we see that  $\phi = U^\dagger e^{i\omega} \Lambda U$  is a *normal* matrix,<sup>3</sup> with eigenvalues  $\text{diag}(e^{i\omega_1} \lambda_1, \dots, e^{i\omega_N} \lambda_N)$ . Thus, normal matrices, or partially normal matrices (i.e., the case  $K < N$ ), evade the “Single Ring” theorem: if the first  $K$  eigenvalues  $\lambda_1^2, \lambda_2^2, \dots, \lambda_K^2$  of  $\phi^\dagger \phi$  split into several disjoint segments along the positive real axis, the corresponding eigenvalues of  $\phi$  will split into concentric annuli in the complex plane obtained by revolving those  $\lambda$ -segments. Normal, or partially normal matrices are, of course, extremely rare in the ensembles of non-hermitean matrices studied in this paper, and do not affect the “Single Ring” behavior of the bulk of matrices in the ensemble.

We end this section by showing how simple features of  $F(w)$  indicate whether the domain of the eigenvalue distribution is a disk or an annulus. As is well known [11, 19, 20], for  $V$  a polynomial of degree  $p$ , the Green’s function  $F(w)$  is given by<sup>4</sup>

$$F(w) = \frac{1}{2}V'(w) - P(w)\sqrt{(w-a)(w-b)}, \quad (2.11)$$

where

$$P(w) = \sum_{k=-1}^{p-2} c_k w^k. \quad (2.12)$$

The real constants  $0 \leq a < b$  and  $c_k$  are then determined completely by the requirement that  $F(w) \rightarrow \frac{1}{w}$  as  $w$  tends to infinity, and by the condition that  $F(w)$  has at most an integrable singularity as  $w \rightarrow 0$ . Thus, if  $a > 0$ , inevitably  $c_{-1} = 0$ . However, if  $a = 0$ , then  $c_{-1}$  will be determined by the asymptotic behavior for  $w$  large.

According to the “Single Ring” theorem [4], the eigenvalue distribution of  $\phi$  is either a disk or an annulus. The behavior of  $F(w)$  as  $w \sim 0$  turns out to be an indicator as to which phase of the two the system is in, as we now show:

---

<sup>3</sup>That is,  $[\phi, \phi^\dagger] = 0$ .

<sup>4</sup>Here we assume for simplicity that the eigenvalues of  $\phi^\dagger \phi$  condense into a single segment  $[a, b]$ . Discussion of condensation of  $\phi^\dagger \phi$  eigenvalues into more segments appears in the Appendix.

*A. Disk Phase:* In the disk phase we expect that  $\rho(0) > 0$ , as in Ginibre's case. Thus, from (2.6)  $\rho(r) = (1/r)(d\gamma/dr) \equiv 2(d\gamma/dr^2)$  and from the first sum rule  $\gamma(0) = 0$  in (2.7) we conclude that

$$\gamma(r) \sim \frac{1}{2}\rho(0)r^2 \quad (2.13)$$

near  $r = 0$ . Therefore, for  $r$  small, (2.10) yields

$$F\left(-\frac{\rho(0)r^4}{2} + \dots\right) \sim -\frac{1}{r^2}, \quad (2.14)$$

namely,  $F(w) \sim 1/\sqrt{w}$  for  $w \sim 0$ , as we could have anticipated from Ginibre's case.<sup>5</sup> This means that in the disk phase we must set  $a = 0$  in (2.11). Consequently, in the disk phase  $c_{-1}$  does not vanish. We can do even better: paying attention to the coefficients in (2.11) and (2.12) (with  $a = 0$ ) we immediately obtain from (2.14) that

$$c_{-1} = \sqrt{\frac{\rho(0)}{2b}}. \quad (2.15)$$

*B. Annular Phase:* In the annular phase  $\gamma(r)$  must clearly vanish identically in the inner void of the annulus. Thus, (2.10) implies that  $F(w)$  cannot have a pole at  $w = 0$ , and therefore from (2.11) we must have  $c_{-1}\sqrt{ab} = 0$ . Thus, the annulus must arise for  $c_{-1} = 0$  (the other possible solution  $a = 0, c_{-1} \neq 0$  leads to a disk configuration with  $\gamma = 0$  only at  $r = 0$ , as we just discussed.)

Thus, to summarize, in the disk phase  $F$  has the form

$$F_{disk}(w) = \frac{1}{2}V'(w) - \left(\sqrt{\frac{\rho(0)}{2b}}w^{-1} + c_0 + c_1 w + \dots + c_{p-2} w^{p-2}\right)\sqrt{w(w-b)}, \quad (2.16)$$

while in the annular phase it has the form

$$F_{annulus}(w) = \frac{1}{2}V'(w) - \left(c_0 + c_1 w + \dots + c_{p-2} w^{p-2}\right)\sqrt{(w-a)(w-b)}. \quad (2.17)$$

---

<sup>5</sup>In the Gaussian case,  $V = \phi^\dagger\phi$ , we have  $2\sqrt{w}F(w) = \sqrt{w} - \sqrt{w-4}$ , whence the roots of (2.10) are  $\gamma = 0, 1$  and  $r^2$ . We note that  $\gamma = 0$  is unphysical,  $\gamma = r^2$  (*i.e.*,  $G = z^*$ ) corresponds to Ginibre's disk[12], and  $\gamma = 1$  is the solution outside the disk.

Having determined  $F(w)$  in this way, i.e., having determined the various unknown parameters in (2.16) or in (2.17), we substitute it into (2.10) and find  $G(z, z^*)$ . We can thus calculate the density of eigenvalues  $\rho(r)$  explicitly for an arbitrary  $V$ .

We now turn to the disk-annulus phase transition. An important feature of this transition is that  $F(w)$  is continuous through it. To see this we argue as follows: By tuning the couplings in  $V$ , we can induce a phase transition from the disk phase into the annular phase, or vice versa. Note, of course, that we can parametrize any point in the disk phase either by the set of couplings in  $V$  or by the set of parameters  $\{c_{-1}, c_0, \dots, c_{p-2}; b\}$  in (2.16). The ‘‘coordinate transformation’’ between these two sets of parameters is encoded in the asymptotic behavior of  $F(w)$ . Similarly, we can parametrize any point in the annular phase either by the set of couplings in  $V$  or by the set of parameters  $\{c_0, c_1 \dots c_{p-2}; a, b\}$  in (2.17). Due to the one-to-one relation (in a given phase, once we have established it is the stable one) between the couplings in  $V$  and the parameters in  $F(w) - \frac{1}{2}V'(w)$  (namely, the  $c_n$ 's and the locations of the branch points of  $F(w)$ ), we can describe the disk-annulus transition in terms of the latter parameters (instead of the couplings in  $V$ ). Clearly, the transition point is reached from the disk phase when  $\rho(0) = 0$ , that is, when  $c_{-1}$  in (2.16) vanishes:

$$c_{-1}^{crit} = 0. \quad (2.18)$$

Similarly, the transition point is reached from the annular phase when the lower branch point  $a$  in (2.17) vanishes. Thus, e.g., in a transition from the disk phase into the annular phase,  $F_{disk}(w)$  in (2.16) would cross-over continuously into  $F_{annulus}(w)$  in (2.17) through a critical form

$$F_{crit}(w) = \frac{1}{2}V'_{crit}(w) - \left(c_0^{crit} + c_1^{crit} w + \dots + c_{p-2}^{crit} w^{p-2}\right) \sqrt{w(w - b^{crit})}. \quad (2.19)$$

The continuity of  $F(w)$  through the transition was demonstrated explicitly in [4] for the quartic ensemble  $V(\phi^\dagger\phi) = 2m^2\phi^\dagger\phi + g(\phi^\dagger\phi)^2$  (see also Section 4).

This discussion obviously generalizes to cases when  $F(w)$  has multiple cuts, which correspond to condensation of the eigenvalues of  $\phi^\dagger\phi$  into many segments. If  $w = 0$

is a branch point of  $F(w)$ , that is, if the lowest cut extends to the origin, we are in the disk phase,

$$F_{disk}(w) = \frac{1}{2}V'(w) - (c_{-1}w^{-1} + c_0 + c_1 w + \cdots + c_{p-2} w^{p-2}) \sqrt{w(w - b_1) \cdots (w - b_n)}, \quad (2.20)$$

with  $0 < b_1 < \cdots < b_n$ . The relation (2.15) then generalizes to

$$c_{-1} = \sqrt{\frac{\rho(0)}{2(-1)^{n+1} \prod_{k=1}^n b_k}}. \quad (2.21)$$

Since  $c_{-1}$  must be real we conclude that such a configuration exists only for  $n$  odd.

If the lowest branch point in  $F(w)$  is positive, we are in the annular phase with

$$F_{annulus}(w) = \frac{1}{2}V'(w) - (c_0 + c_1 w + \cdots + c_{p-2} w^{p-2}) \sqrt{(w - a)(w - b_1) \cdots (w - b_n)}. \quad (2.22)$$

The phase transition would occur when the couplings in  $V(\phi^\dagger \phi)$  are tuned such that  $F_{disk}(w)$  and  $F_{annulus}(w)$  match continuously, as was described in the previous paragraph.

### 3 Boundaries and Boundary Values

Remarkably, with a minimal amount of effort, and based on the mere definition of  $F(w)$  (Eq. (2.8), which we repeat here for convenience)

$$F(w) = \left\langle \frac{1}{N} \text{tr}_{(N)} \frac{1}{w - \phi^\dagger \phi} \right\rangle \equiv \int_0^\infty \frac{\tilde{\rho}(\sigma) d\sigma}{w - \sigma}, \quad (3.1)$$

we are able to derive simple expressions for the location of the boundaries of the eigenvalue distribution and also for the boundary values of  $\rho(r)$  in terms of the moments of  $\tilde{\rho}(\sigma)$ , which, we remind the reader, is the density of eigenvalues for a hermitean matrix problem.

To this end it is useful to rewrite our master formula (2.10) for  $\gamma(r)$  as

$$wF(w) = \gamma \quad (3.2)$$

with

$$w = \frac{\gamma r^2}{\gamma - 1}. \quad (3.3)$$

We start with the outer edge  $r = R_{out}$  (either in the disk phase or in the annular phase.) Near the outer edge  $\gamma \rightarrow 1-$ , and thus  $w \rightarrow -\infty$ . We therefore expand  $F(w)$  in powers of  $1/w$  and obtain from (3.1)-(3.3)

$$\frac{\langle \sigma \rangle}{r^2} + \frac{\gamma - 1}{\gamma r^4} \langle \sigma^2 \rangle + \frac{(\gamma - 1)^2}{\gamma^2 r^6} \langle \sigma^3 \rangle + \dots = \gamma, \quad (3.4)$$

where

$$\langle \sigma^k \rangle = \int_0^\infty \tilde{\rho}(\sigma) \sigma^k d\sigma \quad (3.5)$$

are the moments of  $\tilde{\rho}(\sigma)$  (which is of course normalized to 1.) For the class of models we are interested in here, all the moments  $\langle \sigma^k \rangle$ ,  $k \geq 0$  are clearly finite.<sup>6</sup> Thus, at the outer edge  $r = R_{out}$  (where of course  $\gamma(R_{out}) = 1$ ), all terms with  $\langle \sigma^k \rangle$ ,  $k \geq 2$  drop out of (3.4) and we obtain

$$R_{out}^2 = \langle \sigma \rangle. \quad (3.6)$$

---

<sup>6</sup> $\tilde{\rho}(\sigma) \equiv (1/\pi) \text{Im} F(\sigma - i\epsilon)$  is supported along a finite segment (or segments), and its singularity at  $\sigma = 0$  is no worse than  $\sigma^{-1/2}$ .

Namely,  $R_{out}^2$  is simply the first moment of  $\tilde{\rho}(\sigma)$ .

We now calculate the boundary value  $\rho(R_{out})$ . Approaching  $R_{out}$  from the inside, we substitute  $\gamma = 1 - f$  and  $r^2 = R_{out}^2(1 - \delta)$  (with  $f, \delta \ll 1$ ) in (3.4). After some work we obtain  $f = \frac{\langle \sigma \rangle^2}{\langle \sigma^2 \rangle - \langle \sigma \rangle^2} \delta + \mathcal{O}(\delta^2)$ , namely,

$$\gamma = 1 - \frac{\langle \sigma \rangle^2}{\langle \sigma^2 \rangle - \langle \sigma \rangle^2} \delta + \mathcal{O}(\delta^2). \quad (3.7)$$

Thus, from  $\rho(r) = 2(d\gamma/dr^2)$  (Eq. (2.6)) and (3.6) we find

$$\rho(R_{out}) = \frac{2R_{out}^2}{\langle \sigma^2 \rangle - \langle \sigma \rangle^2}. \quad (3.8)$$

The density  $\rho(R_{out})$  is inversely proportional to the variance of  $\sigma$ !

For the  $\tilde{\rho}(\sigma)$  under consideration here,  $\langle \sigma^2 \rangle$ , and consequently  $\rho(R_{out})$ , are always finite. Outside the boundary  $\rho(r)$  vanishes identically, of course, and thus,  $\rho(r)$  always “falls off a cliff” at the boundary, for all probability distributions of the form (1.1) with  $V$  polynomial. It would be thus interesting to study circularly invariant matrix ensembles  $P(\phi^\dagger \phi)$  such that the eigenvalue distribution  $\tilde{\rho}(\sigma)$  of  $\phi^\dagger \phi$  has a finite  $\langle \sigma \rangle$  but an infinite  $\langle \sigma^2 \rangle$ . Then  $\rho(R_{out})$  would vanish. This would naturally raise the question whether in such situations,  $\rho(r)$  behaves universally near the edge (that is, if near the edge it vanishes like  $(R_{out} - r)^\epsilon$  with  $\epsilon$  being some universal exponent). We do not pursue this question further in this paper.

We now turn to the annular phase, and focus on the inner edge  $r = R_{in}$  of the annulus. According to the discussion at the end of Section 2 (see Eq. (2.17) and the discussion above it),  $a > 0$  in (2.11), and thus  $F(w)$  is analytic in the domain  $|w| < a$ . Expanding (3.1) in powers of  $w$ , we obtain from (3.2)

$$\frac{1 - \gamma}{r^2} - \left\langle \frac{1}{\sigma} \right\rangle = w \left\langle \frac{1}{\sigma^2} \right\rangle + w^2 \left\langle \frac{1}{\sigma^3} \right\rangle + \dots. \quad (3.9)$$

A little above the inner radius, into the annulus, clearly  $\gamma \rightarrow 0$  and  $w \rightarrow 0^-$  in (3.3). Thus, setting  $w = 0$  in (3.9) we obtain

$$\frac{1}{R_{in}^2} = \left\langle \frac{1}{\sigma} \right\rangle. \quad (3.10)$$

$R_{in}^{-2}$  is simply the  $\sigma^{-1}$  moment of  $\tilde{\rho}(\sigma)$ .

We can now calculate the boundary value  $\rho(R_{in})$ . Near the inner edge we parametrize  $r^2 = R_{in}^2(1 + \delta)$  with  $\delta \ll 1$  (and of course,  $\gamma \ll 1$  to begin with.) Since  $\tilde{\rho}(\sigma)$  obviously vanishes for  $\sigma < a$ , all moments  $\langle \sigma^{-k} \rangle$  in (3.9) are finite. Thus, dropping all terms with  $\langle \sigma^{-k} \rangle, k \geq 3$  in (3.9), we obtain after some work

$$\gamma = R_{in}^{-4} \frac{\delta}{\langle \sigma^{-2} \rangle - \langle \sigma^{-1} \rangle^2} + \mathcal{O}(\delta^2). \quad (3.11)$$

It then follows from (2.6) and (3.10) that

$$\rho(R_{in}) = \frac{2R_{in}^{-6}}{\langle \sigma^{-2} \rangle - \langle \sigma^{-1} \rangle^2}. \quad (3.12)$$

The density  $\rho(R_{out})$  is inversely proportional to the variance of  $\sigma^{-1}$ .

From (2.11) (or (2.17)) we learn that in the annular phase  $\tilde{\rho}_{annulus}(\sigma) \equiv \frac{1}{\pi} \text{Im} F(\sigma - i\epsilon) = \text{polynomial}(\sigma) \sqrt{(\sigma - a)(b - \sigma)}$ ,  $0 < a < \sigma < b$  (and vanishes elsewhere.) Thus,  $\langle 1/\sigma^k \rangle \equiv \int_a^b (\tilde{\rho}(\sigma)/\sigma^k) d\sigma$ ,  $k = 1, 2$  are finite. Therefore,  $\rho_{annulus}(\sigma)$  jumps from zero (in the inner void of the annulus) to a finite value at the inner edge  $R_{in}$ . Note, however, that when  $a \rightarrow 0$ , that is, in the annular to disk transition,  $\langle 1/\sigma \rangle$  remains finite, but  $\langle 1/\sigma^2 \rangle$  diverges like  $1/\sqrt{a}$ . (For a particular example see Eq. (4.18).) Thus, from (3.10) we see that  $R_{inner}(a = 0)$ , the *critical* inner radius, is finite. The annulus starts up with a finite inner radius. Also, in this limit, we see from (3.12) that  $\rho(R_{in})$  vanishes like  $\sqrt{a}$ . As we approach the annulus-disk transition, the discontinuity in  $\rho(r)$  at the (finite) inner edge disappears.

We saw at the end of Section 2 (see Eqs. (2.16)-(2.19)) that  $F(w)$  is continuous through the disk-annulus phase transition. Thus, our master formula  $wF(w) = \gamma$  to determine  $\gamma(r)$  (Eq. (3.2)) is also continuous through the transition. Consequently,  $\rho(r) = (1/r)(d\gamma/dr)$  must remain continuous through the disk-annulus transition, and has (at the transition) the universal behavior described in the previous paragraph.

## 4 Phase Transitions in the Quartic Ensemble

The disk-annulus transition in the quartic ensemble

$$V(\phi^\dagger\phi) = 2m^2\phi^\dagger\phi + g(\phi^\dagger\phi)^2 \quad (4.1)$$

was studied in detail in [4]. The annular eigenvalue distribution  $\rho_{annular}(r)$  and the disk eigenvalue distribution  $\rho_{disk}(r)$  for this ensemble were calculated explicitly in [4]. According to the expressions given in [4], as the critical point is approached from the annular phase,  $\rho_{annular}(r)$  behaves precisely as described in the paragraph following Eq. (3.12) at the end of the previous section (see also Eq.(4.13) below, at  $\mu = \mu_c$ .) Also according to [4], as the critical point is approached from the disk phase,  $\rho_{disk}(r)$  gets completely depleted inside a region of radius  $R_{in}(\mu_c)$  (remaining continuous at  $r = R_{in}(\mu_c)$ ). See Eq. (4.20) below.) Thus,  $\rho(r)$  for the quartic ensemble is continuous through the disk-annulus transition.

In this section we verify the expressions (3.6), (3.8), (3.10) and (3.12) for  $R_{out}$ ,  $\rho(R_{out})$ ,  $R_{in}$  and  $\rho(R_{in})$  for the quartic ensemble (4.1) against the explicit expressions for these quantities given in [4], and also provide ample numerical results concerning the disk phase, the annular phase, and the transition between them, in support of the analytical results. In what follows we have omitted many technical details that can be found in [4].

### 4.1 The Disk Phase

For  $m^2 > -\sqrt{2g}$  the density of eigenvalues is a disk. According to [4] we have

$$F(w) = m^2 + gw - \left(\frac{c}{w} + g\right) \sqrt{w(w-b)} \quad (4.2)$$

with

$$c = \frac{2m^2 + \sqrt{m^4 + 6g}}{3}, \quad \text{and} \quad b = \frac{-2m^2 + 2\sqrt{m^4 + 6g}}{3g}. \quad (4.3)$$

According to Eqs. (5.8) and (5.9) in [4], the eigenvalue density in this phase is

$$\rho_{disk}(r) = 2m^2 + 4gr^2 + 2[\text{sgn}\left(\frac{b}{4} - r^2\right)] \frac{bc^2 - (m^2 + 2gr^2)[1 + 2(m^2r^2 + gr^4)]}{\sqrt{[1 + 2(m^2r^2 + gr^4)]^2 - 4bc^2r^2}} \quad (4.4)$$

inside a disk of radius  $R_{out}$ , where

$$R_{out}^2 = \frac{bc^2 - 2m^2}{2g} = \frac{(m^4 + 6g)^{3/2} - m^2(m^4 + 9g)}{27g^2}. \quad (4.5)$$

Thus, from (4.4) and (4.5) we have <sup>7</sup>

$$\rho_{disk}(R_{out}) = \frac{4g(bc^2 - 2m^2)}{2g - bc^2(bc^2 - 2m^2)} = \frac{4gR_{out}^2}{1 - 2R_{out}^2(gR_{out}^2 + m^2)}. \quad (4.6)$$

These results should be compared with the predictions of Section 3. From (4.2) we can read-off the density of eigenvalues  $\tilde{\rho}(\sigma) = (1/\pi)\text{Im}F(\sigma - i\epsilon)$  of  $\phi^\dagger\phi$  as

$$\tilde{\rho}(\sigma) = \frac{1}{\pi} \left( \frac{c}{\sigma} + g \right) \sqrt{\sigma(b - \sigma)} \quad (4.7)$$

for  $0 \leq \sigma \leq b$ , and zero elsewhere. We can readily check that (4.7) is properly normalized to 1.

The first two moments of (4.7) are

$$\langle \sigma \rangle = \frac{1}{2} \left( \frac{b}{2} \right)^2 \left( c + \frac{gb}{2} \right) = \frac{(m^4 + 6g)^{3/2} - m^2(m^4 + 9g)}{27g^2}, \quad (4.8)$$

and

$$\langle \sigma^2 \rangle = \frac{1}{8} \left( \frac{b}{2} \right)^4 \left( \frac{8c}{b} + 5g \right) = \frac{27g^2 + 18gm^4 + 2m^8 - 2m^2(6g + m^4)^{3/2}}{54g^3}. \quad (4.9)$$

Thus,

$$\begin{aligned} \langle \sigma^2 \rangle - \langle \sigma \rangle^2 &= -\frac{b^3}{256} \left[ 4bc^2 + bg(b^2g - 10) + 4c(b^2g - 4) \right] \\ &= \frac{297g^3 + 108g^2m^4 - 18gm^8 - 4m^{12} - 2m^2(9g - 2m^4)(6g + m^4)^{3/2}}{1458g^4}. \end{aligned} \quad (4.10)$$

Comparing (4.5) and (4.8) we immediately verify (3.6),  $R_{out}^2 = \langle \sigma \rangle$ . After some additional work, using (4.10) and (4.5) in (3.8), we can see that (3.8), namely, that  $\rho(R_{out}) = 2R_{out}^2 / (\langle \sigma^2 \rangle - \langle \sigma \rangle^2)$ , coincides with (4.6).

<sup>7</sup>It is straight forward to show that  $\text{sgn}(\frac{b}{4} - R_{out}^2) = -1$  in (4.4): just substitute  $m^4 = A^2 \cos^2 \alpha$  and  $6g = A^2 \sin^2 \alpha$  and obtain that  $R_{out}^2 - \frac{b}{4} = (A^3/108g^2)(1 - \cos \alpha)^3$ .

### 4.1.1 Numerical Results for the Disk Phase

We have generated numerically random matrix ensembles corresponding to the quartic potential (4.1) in the disk phase, for  $m^2 = 1$  fixed and for various values of the coupling  $g$  (and for various sizes of matrices), and measured  $\rho_{disk}(r)$  for these realizations.

The generation of the matrices was done by a standard Metropolis Monte Carlo approach. A random change had been suggested in the real and imaginary parts of one of the elements of  $\phi$  and then the change in  $V(\phi)$  was evaluated. This “move” was accepted unconditionally if  $V$  were decreased, and with probability  $p = e^{-\Delta V}$  if  $V$  were increased. General theorems on Monte Carlo then guaranteed that the resulting probability distribution of  $\phi$  was the desired one. After the matrices were generated, their eigenvalues were determined with a standard solver from the LAPACK library. We tuned the size of the suggested changes in  $\phi$  so that the acceptance rate was about one-half, and monitored the equilibration and autocorrelation times to ensure our starting configuration had evolved properly and error bars have were accurate. In particular, the local changes in  $\phi$  made the matrices correlated over some number of random changes, however, local changes also allowed one to employ various tricks to evaluate the change in  $V$  rapidly.

In Figure 1 we display our numerical results for  $\rho_{disk}(r)$  for 128x128 dimensional matrices, and compare them to the analytical large- $N$  result (4.4) of [4]. (As a trivial check of our numerical code, we also included in this figure the results for the gaussian (Ginibre) ensemble.)

Evidently, the agreement between the numerical and the analytical results is good. Note the finite- $N$  effects near the edge of the disk.

## 4.2 The Annular Phase

For  $m^2 < -\sqrt{2g}$ , the stable eigenvalue distribution is annular. For convenience, let us switch notations according to  $m^2 = -\mu^2$ , and also write  $\mu_c^2 = \sqrt{2g}$ .

According to [4] we have

$$F(w) = m^2 + gw - g \sqrt{(w-a)(w-b)} \quad (4.11)$$

with

$$a = \frac{\mu^2}{g} - \sqrt{\frac{2}{g}}, \quad \text{and} \quad b = \frac{\mu^2}{g} + \sqrt{\frac{2}{g}}. \quad (4.12)$$

We see that  $a = (2/\mu_c^4)(\mu^2 - \mu_c^2)$  which is positive for  $\mu^2 > \mu_c^2$ , as it should be, by definition.

According to Eqs. (5.16) - (5.19) in [4], the eigenvalue density in this phase is

$$\rho_{annulus}(r) = 8g \left( r^2 - \frac{\mu^2}{2g} \right) = 8g \left( r^2 - \frac{\mu^2}{\mu_c^4} \right) \quad (4.13)$$

inside an annulus  $R_{in} \leq r \leq R_{out}$ , where

$$R_{in}^2 = \frac{\mu^2 + \sqrt{\mu^4 - 2g}}{2g} = \frac{\mu^2 + \sqrt{\mu^4 - \mu_c^4}}{\mu_c^4} \quad (4.14)$$

and

$$R_{out}^2 = \frac{\mu^2}{g} = \frac{2\mu^2}{\mu_c^4}. \quad (4.15)$$

Thus, we see immediately that

$$\begin{aligned} \rho(R_{in}) &= 4\sqrt{\mu^4 - \mu_c^4} \\ &\text{and} \\ \rho(R_{out}) &= 4\mu^2. \end{aligned} \quad (4.16)$$

Note that  $\rho(R_{in}) = 0$  at  $\mu = \mu_c$ , as expected. Also note that the critical annulus has a finite inner radius:  $R_{in}^2(\mu_c) = 1/\mu_c^2 > 0$ .

We now compare these results with the predictions of Section 3. From (4.11) we read-off the density of eigenvalues of  $\phi^\dagger\phi$ :

$$\tilde{\rho}(\sigma) = \frac{g}{\pi} \sqrt{(\sigma-a)(b-\sigma)} \quad (4.17)$$

for  $a \leq \sigma \leq b$ , and zero elsewhere. We can check that (4.17) is properly normalized to 1.

The relevant moments of (4.17) are

$$\begin{aligned}
\langle \sigma \rangle &= \frac{g}{2} \left( \frac{a+b}{2} \right) \left( \frac{b-a}{2} \right)^2 = \frac{\mu^2}{g} \\
\langle \sigma^2 \rangle &= \frac{g}{2} \left( \frac{b-a}{2} \right)^4 \left[ \left( \frac{b+a}{b-a} \right)^2 + \frac{1}{4} \right] = \frac{\mu^4}{g^2} + \frac{1}{2g} \\
\langle \frac{1}{\sigma} \rangle &= \frac{g}{2} (\sqrt{b} - \sqrt{a})^2 = \mu^2 - \sqrt{\mu^4 - 2g} \\
&\text{and} \\
\langle \frac{1}{\sigma^2} \rangle &= \frac{g (\sqrt{b} - \sqrt{a})^2}{2 \sqrt{ab}} = g \frac{\mu^2 - \sqrt{\mu^4 - 2g}}{\sqrt{\mu^4 - 2g}}. \tag{4.18}
\end{aligned}$$

Comparing (4.14), (4.15) and the first and third equations in (4.18), we verify (3.6) and (3.10) straightforwardly.

Further, we find from (4.18) that

$$\begin{aligned}
\langle \sigma^2 \rangle - \langle \sigma \rangle^2 &= \frac{1}{2g} \\
&\text{and} \\
\langle \frac{1}{\sigma^2} \rangle - \langle \frac{1}{\sigma} \rangle^2 &= g - 2\mu^4 + \mu^2 \frac{2\mu^4 - 3g}{\sqrt{\mu^4 - 2g}}. \tag{4.19}
\end{aligned}$$

Thus, comparing with (4.16) we find that

$$\frac{2R_{out}^2}{\langle \sigma^2 \rangle - \langle \sigma \rangle^2} = 4\mu^2 = \rho(R_{out})$$

and

$$\frac{2R_{in}^{-6}}{\langle \sigma^{-2} \rangle - \langle \sigma^{-1} \rangle^2} = 4\sqrt{\mu^4 - \mu_c^4} = \rho(R_{in}),$$

and verify (3.8) and (3.12) for the annular phase.

#### 4.2.1 Numerical Results for the Annular Phase

In Figures 2.a-2.c we display our numerical results for  $\rho_{annulus}(r)$  for matrices of various sizes, and compare them to the analytical large- $N$  result (4.13) of [4]. In these figures we hold  $\mu^2 = 0.5$  fixed, and increase  $g$  from 0.025 to 0.1<sup>8</sup>.

<sup>8</sup>Here we have  $\mu^2 = 0.5 = \mu_c^2/2\sqrt{2g}$ . Thus increasing  $g$  as indicated in the text brings us closer to the disk-annulus phase transition.

### 4.3 The Disk-Annulus Phase Transition

The phase boundary separating the disk phase and the annular phase in the  $m^2 - g$  plane is the curve  $m^2 = -\sqrt{2g}$ .

Consider approaching this boundary from within the disk phase by setting  $m^2 = -\sqrt{2g} + \delta$ , with  $\delta$  positive and small. Then, using (4.3), we find to first order in  $\delta$  that  $c = \delta/2$  and  $b = 2\sqrt{(2/g)} - \delta/g$ . In particular, at the phase boundary itself  $c = 0$ , in accordance with (2.18) and (2.19). It was shown in [4] that as one approaches the critical point  $m^2 = -\sqrt{2g}$  from the disk phase, the density of eigenvalues of  $\phi$  approaches the particularly simple critical configuration

$$\rho_{crit}(r) = \begin{cases} 0 & , \quad r^2 < 1/\sqrt{2g} \\ 8g(r^2 - \frac{1}{\sqrt{2g}}) & , \quad 1/\sqrt{2g} < r^2 < \sqrt{2/g}, \end{cases} \quad (4.20)$$

Thus, as we decrease  $\delta$  to zero,  $\rho_{disk}(r)$  (Eq. (4.4)) becomes increasingly depleted inside the disk  $r^2 < b(\delta)/4$ , reaching complete depletion at  $\delta = 0$ , at which point the disk breaks into an annulus. We also note that at the phase boundary (4.2) reads

$$F(w) = -\sqrt{2g} + gw - g \sqrt{w \left( w - 2\sqrt{\frac{2}{g}} \right)}. \quad (4.21)$$

Consider now approaching the phase boundary  $m^2 = -\sqrt{2g}$  from within the annular phase. Thus, we set  $\mu^2 = \sqrt{2g} + \delta$ , with  $\delta$  positive and small. Then, since all the expressions in (4.12) are linear in  $\mu^2$ , we find that  $a = \delta/g$  and  $b = 2\sqrt{(2/g)} + \delta/g$ . In particular, at the phase boundary itself  $a = 0$ , and  $b = 1/\sqrt{2g}$ . Therefore, at the phase boundary (4.11) reads

$$F(w) = -\sqrt{2g} + gw - g \sqrt{w \left( w - 2\sqrt{\frac{2}{g}} \right)},$$

which coincides with (4.21). Thus,  $F(w)$  (and consequently, the eigenvalue density of  $\phi^\dagger\phi$ ) is also continuous at the transition, in accordance with (2.19).

Note from (4.14) and (4.15) that at the transition  $R_{in}^2 = 1/\mu_c^2 = 1/\sqrt{2g}$  is *finite*, and coincides with the radius (squared) of the depleted region in the disk configuration

(4.20). Right at the transition, the disk breaks into an annulus with a finite hole! Note also that  $R_{out}^2 = 2/\mu_c^2 = \sqrt{2/g}$ , which coincides with the disk's  $R_{out}^2$  at the phase boundary. Thus, at the phase boundary  $\mu^2 = \mu_c^2$  (4.13) coincides with (4.20), namely,  $\rho(r)$  is continuous at the transition from the disk phase to the annular phase.

### 4.3.1 Numerical Simulation of the Disk-Annulus Phase Transition

We have measured the density of eigenvalues  $\rho(r)$  of matrices  $\phi$  of size 128x128, taken from the the quartic ensemble with  $\mu^2 = 0.5$  and for  $g = 0.025, 0.05, 0.1, 0.125, 0.15$  and 0.175. The results are displayed on Figure 3.

For these values of  $g$ , we start in the annular phase at the lowest value of  $g$ . For our set of parameters we have  $\mu^2 = 0.5 = \mu_c^2/2\sqrt{2g}$ . Thus, increasing  $g$  (while keeping  $\mu^2$  fixed at 0.5) brings us closer to the disk-annulus phase transition, which occurs (at large  $N$ ) at  $g_c = 0.125$ . Increasing  $g$  beyond that, puts us into the disk phase.

The first three profiles on the right in Figure 3 belong to the annular phase. Their behavior is consistent with our discussion in Section 4.2 of the annular phase. Indeed, as  $g$  increases towards the transition point at  $g_c = 0.125$ , these three graphs exhibit the expected decrease of  $R_{in}^2 = (\mu^2 + \sqrt{\mu^4 - \mu_c^4})/\mu_c^4$  (Eq. (4.14), with  $\mu_c^2 = \sqrt{2g}$ ) and the decrease of  $R_{out}^2 = 2\mu^2/\mu_c^4$  (Eq. (4.15)).

The critical density profile, corresponding to  $g_c = 0.125$ , is the fourth profile (from the right). For our choice of parameters, the theoretical boundary radii of the critical annulus, i.e., at  $g = 0.125$ , are  $R_{in}^{crit} = 1/\mu_c = \sqrt{2}$  and  $R_{out}^{crit} = \sqrt{2}/\mu_c = 2$ . These boundary values fit nicely with the features of the critical profile in Figure 3.

Finally, the last two profiles in Figure 3 have pronounced tails extending to  $r = 0$  and thus belong to the disk phase.

## 5 Phase Transitions in the Sixth Order Potential and the “Single Ring” Theorem

The sextic potential

$$V(\phi^\dagger\phi) = m^2\phi^\dagger\phi + \frac{\lambda}{2}(\phi^\dagger\phi)^2 + \frac{g}{3}(\phi^\dagger\phi)^3 \quad (5.1)$$

is the potential of lowest degree in (1.1) for which the eigenvalues of  $\phi^\dagger\phi$  may split into more than a single segment. In fact, it is easy to see that there can be at most two eigenvalue segments in the spectrum of  $\phi^\dagger\phi$ .

The qualitative features of the support of the eigenvalue density associated with (5.1) can be deduced by moving the cubic  $V(x) = m^2x + \frac{\lambda}{2}x^2 + \frac{g}{3}x^3$  around in the plane (i.e., by varying its couplings, fixing, say  $g = 1$ ), and concentrating on  $x \geq 0$ . It is obvious from such considerations that there are three qualitatively different phases in the spectrum of  $\phi^\dagger\phi$ . In two of the phases the eigenvalues  $s_i$  of  $\phi^\dagger\phi$  live in a single segment. In one of these single segment phases, the segment includes the origin ( $0 \leq s \leq a$ ), but in the other it does not ( $0 < a \leq s \leq b$ ). Following the general discussion in the last part of Section 2, we would expect that the spectrum of  $\phi$  itself is a disk in the first case, and an annulus in the second case.

In the third phase of  $\phi^\dagger\phi$ , there are two segments, one of which hits the origin ( $\{0 \leq s \leq a\} \cup \{b \leq s \leq c\}$ ). (There is no two-segment phase of  $\phi^\dagger\phi$  which does not include the origin.) Thus, according to the discussion in the last part of Section 2, the non-hermitean matrix  $\phi$  is expected to be in the disk phase in this case (rather than having its eigenvalue fill in a disk surrounded by a concentric annulus), in accordance with the “Single Ring” theorem.

In this short section we limit our discussion to the two-segment phase of  $\phi^\dagger\phi$ . (A rather detailed sketch of the analytical conditions that determine the whole phase structure of the sextic ensemble (5.1) is given in the Appendix.) Our purpose here is to demonstrate numerically the “Single Ring” Theorem for the eigenvalue distribution of matrices  $\phi$  taken from the sextic ensemble (5.1). To this end, we have to identify points well within the phase in which the eigenvalues of  $\phi^\dagger\phi$  split into two segments.

We used the formalism of the Appendix to choose two ensembles in the two-segment phase of  $\phi^\dagger\phi$ , for which we verified that the eigenvalues of  $\phi$  formed a disk. The results for these ensembles are displayed in Figures 4 and 5.

Figure 4 shows the scatter plot of the eigenvalues of  $\phi$  together with the density of eigenvalues  $\tilde{\rho}(s)$  of  $\phi^\dagger\phi$  for (5.1) with couplings  $m^2 = 7.372$ ,  $\lambda = -6.116$  and  $g = 1.372$ . As can be seen on the right part of Figure 4, for these couplings, the eigenvalues of  $\phi^\dagger\phi$  live in two separated segments:  $\{0 \leq s \leq a = 1\} \cup \{b = 2 \leq s \leq c = 3\}$ . The solid line there is the large  $N$  theoretical curve, which was plotted according to the analysis we have described in the Appendix (see the discussion following (A.20)). Evidently, the spectrum of  $\phi$  is a disk, despite the split support of  $\tilde{\rho}(s)$ , in accordance with the “Single Ring” Theorem.

Figure 5 is similar to Figure 4, but for (5.1) with couplings  $m^2 = 6.403$ ,  $\lambda = 4.184$  and  $g = 0.713$ , for which the eigenvalues of  $\phi^\dagger\phi$  live in the segments  $\{0 \leq s \leq a = 1\} \cup \{b = 3 \leq s \leq c = 4\}$ . The spectrum of  $\phi$  remains a disk, even though the two segments of the support of  $\tilde{\rho}(s)$  are more separated than in Figure 4.

# Appendix A The Phase Diagram of a Generic $V(\phi^\dagger\phi)$

In this Appendix we briefly review the necessary theoretical aspects of multi-cut phases of  $\phi^\dagger\phi$ . The first part of our discussion will apply for a generic polynomial  $V(\phi^\dagger\phi)$ . Then, in the second part of the Appendix, we will specialize to the sextic potential (5.1).

For practical reasons, we eliminate some (or all) of the couplings in  $V(\phi^\dagger\phi)$  in terms of the end-points of the segments containing the eigenvalue distribution of  $\phi^\dagger\phi$ , and use the latter as (part of) the coordinates in the phase diagram. In this way we can find rather easily which couplings in  $V(\phi^\dagger\phi)$  are needed to generate an eigenvalue distribution of  $\phi^\dagger\phi$  with a prescribed set of support segments.

## A.1 A generic potential $V(\phi^\dagger\phi)$

The saddle-point equation governing the Dyson gas of eigenvalues of  $\phi^\dagger\phi$  is [19, 20]

$$\operatorname{Re}F(s - i\epsilon) = \frac{1}{2}V'(s). \quad (\text{A.1})$$

By definition (see Eq. (2.8))

$$F(w) = \frac{1}{N} \langle \operatorname{tr}_{(N)} \frac{1}{w - \phi^\dagger\phi} \rangle = \frac{1}{N} \sum_{i=1}^N \langle \frac{1}{w - s_i} \rangle \quad (\text{A.2})$$

(where  $s_i$  are the eigenvalues of  $\phi^\dagger\phi$ ). Thus, as usual,

$$F(s - i\epsilon) = \text{P.P.} \frac{1}{N} \sum_{j=1}^N \langle \frac{1}{s - s_j} \rangle + i\pi\tilde{\rho}(s), \quad (\text{A.3})$$

where  $\tilde{\rho}(s)$  is the density of eigenvalues of  $\phi^\dagger\phi$ .

In order to study multi-cut configurations of  $\tilde{\rho}(s)$ , we also need the auxiliary function [21]

$$G(s) = \int_{a_1 > 0}^s d\mu (V'(\mu) - 2F(\mu - i\epsilon)). \quad (\text{A.4})$$

In the last equation  $a_1$  is the lowest branch point of  $F(w)$ . Thus, from (A.3) and (A.1), we see that for  $s$  real and in the support of eigenvalues,

$$G(s) = -2\pi i \int_{a_1}^s \tilde{\rho}(\mu) d\mu \quad (\text{A.5})$$

is pure imaginary.  $-\text{Im } G(s) = 2\pi\tilde{\rho}(s)$  is then positive and monotonically increasing (and reaches  $2\pi$  when  $s$  hits the largest branch point).

*Stability of multi-cut distributions* How do we know that a given distribution of eigenvalues is stable against migration of eigenvalues from one place to another? To answer this question, consider the Dyson gas energy functional

$$S_{eff}[\tilde{\rho}] = \int_{s \geq 0} \tilde{\rho}(s) V(s) ds - \frac{1}{2} \int_{s, \mu \geq 0} \tilde{\rho}(s) \tilde{\rho}(\mu) \log(s - \mu)^2 ds d\mu. \quad (\text{A.6})$$

A general variation of (A.6) under  $\tilde{\rho}(s) \rightarrow \tilde{\rho}(s) + \delta\tilde{\rho}(s)$  is

$$\delta S_{eff}[\tilde{\rho}] = \int_{s \geq 0} V(s) \delta\tilde{\rho}(s) ds - \int_{s, \mu \geq 0} \tilde{\rho}(\mu) \log(s - \mu)^2 \delta\tilde{\rho}(s) ds d\mu. \quad (\text{A.7})$$

Moving an eigenvalue from  $s_i$  to  $s_f$  corresponds to  $\delta\tilde{\rho}(s) = (1/N)[\delta(s - s_f) - \delta(s - s_i)]$ . Thus, from (A.7) and (A.4) (and after some work) we can show that such a move costs

$$\Delta S_{eff}[\tilde{\rho}] = \frac{1}{N} [G(s_f) - G(s_i)] \quad (\text{A.8})$$

in energy [21]. Such a rearrangement of eigenvalues costs energy only if

$$\text{Re } \Delta S_{eff}[\tilde{\rho}] > 0, \quad (\text{A.9})$$

and therefore (A.9) is the stability condition against such a rearrangement. Thus, a multi-cut  $F(w)$ , where the eigenvalues coalesce into  $n$  segments

$$[a_1, a_2] \cup [a_3, a_4] \cup \cdots \cup [a_{2n-1}, a_{2n}],$$

would be stable against migration of eigenvalues between neighboring cuts if and only if (A.9) would hold for all neighboring pairs of cuts, and in both directions. Since

$G(s)$  is real on the segments on the real axis that connect the cuts, this stability condition means

$$G(a_3) = G(a_2), G(a_5) = G(a_4), \dots G(a_{2n-1}) = G(a_{2n-2}). \quad (\text{A.10})$$

In addition, of course,  $\text{Re } G(s) < 0$  cannot happen anywhere for  $s \geq 0$ . The  $n - 1$  equations (A.10) comprise the desired stability condition for such an eigenvalue distribution. In addition to these conditions, we have to make sure that along the cuts themselves  $-\text{Im } G(s) > 0$ , which is just the condition that  $\tilde{\rho}(s)$  be positive.

The  $n - 1$  equations (A.10), together with the obvious analytic properties of  $F(w)$  and its asymptotic behavior

$$F(w) \sim \frac{1}{w} \quad (\text{A.11})$$

as  $w \rightarrow \infty$ , determine  $F(w)$  uniquely. Indeed, as is well known, for a generic  $V(\phi^\dagger \phi)$ , in view of (A.1) and (A.11) (and as we discussed at the end of Section 2),  $F(w)$  (with  $n$  cuts) must be of the form

$$F(w) = \frac{1}{2}V'(w) - P(w)\sqrt{\prod_{l=1}^{2n}(w - a_l)}, \quad (\text{A.12})$$

where

$$P(w) = \frac{c_{-1}}{w} + \sum_{l=0}^{\deg V - n - 1} c_l w^l. \quad (\text{A.13})$$

Here  $a_1 < a_2 \dots < a_{2n}$  and  $c_{-1} \neq 0$  only if  $a_1 = 0$  (see Section 2). If  $a_1 > 0$ , then  $c_{-1} = 0$ , and thus in such a case, there are  $2n(a's) + (\deg V - n)(c's) = n + \deg V$  independent parameters in the expression (A.12) for  $F(w)$ . On the other hand, there are  $\deg V + 1$  conditions from the asymptotic behavior (A.11) plus additional  $n - 1$  conditions from (A.10), which comprise a total of  $\deg V + n$  conditions, equal to the number of unknown parameters. This balance remains if  $c_{-1}$  appears in the game as an unknown parameter, because then  $a_1 = 0$ , so that the number of parameters does not change. Finally, we have to remember to impose the positivity constraint

$$\tilde{\rho}(x) = \frac{1}{\pi} \text{Im } F(x - i\epsilon) \geq 0, \quad (\text{A.14})$$

which translates into a set of inequalities among the  $a$ 's and  $c$ 's.

*A convenient local parametrization of the phase diagram* Recall, that the phases of  $\phi^\dagger\phi$  are specified by the number of segments in the support of  $\tilde{\rho}(s)$ , i.e., the number of cuts in  $F(w)$  (and whether these cuts have  $w = 0$  as a branch point or not.) Thus, instead of the usual description of the phase structure in terms of the  $\text{deg}V$  couplings in  $V(\phi^\dagger\phi)$ , our strategy is to use  $\text{deg}V$  parameters out of the  $2n$  branch-points  $a_1, \dots, a_{2n}$  of  $F(w)$  and the  $\text{deg}P$  coefficients  $c_k$  (with the total number  $\text{deg}V$  first saturated by the  $a$ 's in ascending order), which we refer to as “*phase coordinates*”, to express (in a given phase) the couplings appearing in  $V(\phi^\dagger\phi)$  (such as  $m^2, \lambda$  and  $g$  in (5.1)), as well the  $c_k$ 's and  $a_k$ 's complementary to the phase coordinate parameter set. (See our discussion of the sextic potential below for concrete examples of this parametrization.)

We have to be careful in giving the expressions for, say, the couplings of  $V$ , in terms of the phase coordinates. This because for a given configuration of  $F(w)$ , the equations from which we are to eliminate the couplings of  $V$  (such as the triad  $m^2, \lambda$  and  $g$  in (5.1)) as functions of the phase coordinates may have several solutions (in other words, the couplings in  $V$  are generally multivalued functions of the phase coordinates in a given phase). Thus, in a given phase, we must of course choose the parametrization of couplings in  $V$  which yields the minimal  $S_{eff}[\tilde{\rho}]$  appropriate for that phase.

This alternative parametrization is more convenient for our purposes in Section 5. Indeed, once we are successful in expressing the couplings in  $V$  as functions of the phase coordinates, it will be very easy for us to tune the couplings in  $V(\phi^\dagger\phi)$  to a generic point in a given phase and also to approach the phase boundaries in a controlled manner. In particular, phase transitions appear here, for example, when branch points collide and become equal (at some common real positive value  $a$ ). This process removes 2  $a$ 's and thus closes one cut ( $n \rightarrow n - 1$ ) but adds an additional term to  $P(w)$ . The number of unknown parameters drops by 1, but so does the number of stability conditions (A.10). In the other direction, we can obviously reach

the same coexistence point, by tuning the parameters of  $P(w)$  to a point where it develops a linear factor  $(w - a) = \sqrt{(w - a)^2}$  (with  $a \geq 0$ ). Obviously, when these alternative phase coordinates approach a point on the coexistence surface from two different sides of the phase transition, the respective sets of couplings of  $V$ , expressed as sets of functions of the two phase coordinate patches, coincide. Thus, they lead to the same  $S_{eff}[\tilde{\rho}]$ , which means that such a point is indeed a point on the phase boundary.

## A.2 Results for the sextic potential

From (A.12) and (5.1), the general form of  $F(w)$  is

$$F(w) = \frac{1}{2} (m^2 + \lambda w + gw^2) - P(w) \sqrt{\text{polynomial}}. \quad (\text{A.15})$$

**A. single cut, disk phase:** Here

$$F(w) = \frac{1}{2} (m^2 + \lambda w + gw^2) - \left( \frac{s}{w} + t + uw \right) \sqrt{w(w - a)}. \quad (\text{A.16})$$

There is a single cut, so (A.10) is trivial in this case, and (A.14) holds manifestly. We need only impose (A.11). In the end, we find

$$\begin{aligned} u &= \frac{16 - 8as - 2a^2t}{a^3} \\ g &= 2u \\ \lambda &= 2t - au = \frac{4a^2t + 8as - 16}{a^2} \quad \text{and} \\ m^2 &= 2s - at - \frac{a^2u}{4} = \frac{8as - a^2t - 8}{2a}. \end{aligned} \quad (\text{A.17})$$

The phase coordinates are  $a$ ,  $t$  and  $s$ .

**B. single cut, annular phase:** We have

$$F(w) = \frac{1}{2} (m^2 + \lambda w + gw^2) - (t + uw) \sqrt{(w - a)(w - b)}. \quad (\text{A.18})$$

Here  $0 < a < b$ . Again, there is a single cut, so (A.10) is trivial in this case too, and also (A.14) holds manifestly. We need only impose (A.11). In the end, we find

$$u = \frac{16 - 2t(a - b)^2}{(a + b)(a - b)^2}$$

$$\begin{aligned}
g &= 2u \\
\lambda &= 2t - u(a+b) = 4t - \frac{16}{(a-b)^2} \quad \text{and} \\
m^2 &= -\frac{(a-b)^2}{4}u - t(a+b) = -\frac{4}{a+b} - t\frac{a^2+6ab+b^2}{2(a+b)}. \tag{A.19}
\end{aligned}$$

The phase coordinates are  $a, b$  and  $t$ .

**C. two cuts, disk phase:** We have

$$F(w) = \frac{1}{2} \left( m^2 + \lambda w + g w^2 \right) - \left( \frac{s}{w} + t \right) \sqrt{w(w-a)(w-b)(w-c)}. \tag{A.20}$$

Here  $0 < a < b < c$ . Note that in this case we can trade the three couplings  $m^2, \lambda$  and  $g$  for the three branch points  $a, b$  and  $c$ . In this case there are two cuts, so for the first time (A.10) is not trivial. We first impose (A.11). We find

$$\begin{aligned}
s &= \frac{8}{a^2 + b^2 + c^2 - 2(ab + ac + bc)} \\
&- \frac{1}{2} \frac{a^3 + b^3 + c^3 - a^2(b+c) - b^2(a+c) - c^2(a+b) + 2abc}{a^2 + b^2 + c^2 - 2(ab + ac + bc)} t \\
g &= 2t \\
\lambda &= 2s - t(a+b+c) \quad \text{and} \\
m^2 &= -(a+b+c)s - \frac{a^2 + b^2 + c^2 - 2(ab + ac + bc)}{4} t. \tag{A.21}
\end{aligned}$$

We have yet to impose (A.10), which is why  $t$  was not eliminated yet. Before doing that, we impose (A.14). Our conventions are always to take each cut from the appropriate branch point to the left on the real axis. Thus, after some work, we find from (A.20)

$$\begin{aligned}
\pi \tilde{\rho}(x) &= \text{Im } F(x - i\epsilon) = \\
&\begin{cases} -\left(\frac{s}{x} + t\right) \sqrt{x(a-x)(b-x)(c-x)} & 0 < x < a \\ +\left(\frac{s}{x} + t\right) \sqrt{x(x-a)(x-b)(c-x)} & b < x < c \\ 0 & \text{otherwise.} \end{cases} \tag{A.22}
\end{aligned}$$

We have to impose (A.14) on (A.22). This means

$$\begin{aligned} \frac{s}{x} + t < 0 & \quad \text{for } 0 < x < a \\ & \quad \text{and} \\ \frac{s}{x} + t > 0 & \quad \text{for } b < x < c. \end{aligned}$$

Thus, we must have<sup>9</sup>

$$t > 0 \quad \text{and} \quad -bt \leq s \leq -at < 0, \quad (\text{A.23})$$

where  $s$  is given in (A.21). We are now ready to impose (A.10). Here it simply means  $G(a) = G(b)$ , namely,

$$\int_a^b \left(\frac{s}{x} + t\right) \sqrt{x(x-a)(b-x)(c-x)} dx = 0. \quad (\text{A.24})$$

Note from (A.23) that  $-b < s/t < -a$ , and thus the factor multiplying the square root in (A.24) flips its sign in the integration domain, so that the integral on the LHS of (A.24) may vanish. The latter equation may be expressed in terms of the elliptic integrals

$$\begin{aligned} I(a, b, c) &= \int_a^b \sqrt{x(x-a)(x-b)(x-c)} dx \\ &\quad \text{and} \\ J(a, b, c) &= \int_a^b \sqrt{x(x-a)(x-b)(x-c)} \frac{dx}{x}. \end{aligned} \quad (\text{A.25})$$

Following the usual procedure, we may express  $I$  and  $J$  in terms of complete elliptic integrals in a straightforward manner. (We do not bother to write these expressions here, since for our purposes in Section 5 we evaluated  $I$  and  $J$  numerically.)

Finally, substituting these expressions in (A.24) we obtain

$$s(t, a, b, c)J(a, b, c) + tI(a, b, c) = 0 \quad (\text{A.26})$$

---

<sup>9</sup>It is straightforward to check that the following inequalities hold for the ensembles corresponding to Figures 4 and 5 in Section 5.

which we solve for  $t$  (recall from (A.21) that  $s$  is merely linear in  $t$ , and also that  $t > 0$ , in view of (A.23).) Once  $t(a, b, c)$  is known, we can go back to (A.21) and evaluate  $m^2(a, b, c)$ ,  $\lambda(a, b, c)$  and  $g(a, b, c)$  explicitly. Our phase coordinates in this case are thus  $a, b$  and  $c$ .

### ACKNOWLEDGEMENTS

We thank H. Orland for clarifying the Abstract. The work of A.Z. was supported in part by the National Science Foundation under Grant No. NSF-PHY99-07949. RTS acknowledges M. Papas and support from NSF-DMR-9985978 and also the ITP at UC Santa-Barbara for its hospitality, where part of this work was done. JF's research has been supported in part by the Israeli Science Foundation grant number 307/98 (090-903).

## References

- [1] F. Haake, F. Izrailev, N. Lehmann, D. Saher and H. J. Sommers, *Zeit. Phys. B* **88** (1992) 359.
- H. J. Sommers, A. Crisanti, H. Sompolinsky and Y. Stein, *Phys. Rev. Lett.* **60** (1988) 1895.
- M. A. Stephanov, *Phys. Rev. Lett.* **76** (1996) 4472 . M. A. Halasz, A. D. Jackson and J. J. M. Verbaarschot, *Phys. Rev. D* **56** (1997) 5140; M. A. Halasz, J. C. Osborn and J. J. M. Verbaarschot, *Phys. Rev. D* **56** (1997) 7059. M.A. Halasz, A.D. Jackson, R.E. Shrock, M.A. Stephanov and J.J.M. Verbaarschot, *Phys. Rev. D* **58** (1998) 096007 (hep-ph/9804290).
- T. Guhr and T. Wettig, *Nucl. Phys. B* **506** (1997) 589 (hep-th/9704055); H. Markum, R. Pullirsch and T. Wettig, *Phys. Rev. Lett.* **83** (1999) 484 (hep-lat/9906020).
- R. A. Janik, M. A. Nowak, G. Papp and I. Zahed, *Phys. Rev. Lett.* **77** (1996) 4876. E. Gudowska-Nowak, G. Papp and J. Brickmann, preprint cond-mat/9701187.
- Y. V. Fyodorov, B. A. Khoruzhenko and H.-J. Sommers, *Phys. Rev. Lett.* **79** (1997) 557; *Phys. Lett A* **226** (1997) 46; *Ann. Inst. H. Poincare* **68** (1998) 449; H.-J.Sommers, Yan V. Fyodorov and M.Titov, *J. Phys. A-Math. Gen.* **32** (1999) L77 (chao-dyn/9807015); B. A. Khoruzhenko *Jour. Phys. A. (Math. Gen.)* **29** (1996) L165.
- N. Hatano and D. R. Nelson, *Phys. Rev. Lett.* **77** (1997) 570 (cond-mat/9603165); *Phys. Rev. B* **56** (1997) 8651 (cond-mat/9705290); *Phys. Rev. B* **58** (1998) 8384 (cond-mat/9805195).
- D. R. Nelson and N. M. Shnerb, cond-mat/9708071, *Phys. Rev. Lett.* **80** (1998) 5172 (cond-mat/9801111.); R. A. Lehrer and D. R. Nelson, *Phys. Rev. B* **58** (1998) 12385 (cond-mat/9806016); K. A. Dahmen, D. R. Nelson and N. M. Shnerb, cond-mat/9903276;
- K. B. Efetov, *Phys. Rev. Lett.* **79** (1997) 491; *Phys. Rev. B* **56** (1997) 9630.

A. V. Kolesnikov and K. B. Efetov, *Waves in Random Media* **9** (1999) 71; *Phys. Rev. Lett.* **84** (2000) 5600 (cond-mat/0001263)

J. Feinberg and A. Zee, *Phys. Rev.* **E 59** (1999) 6433 (cond-mat/9706218), *Nucl. Phys.* **B 552** (1999) 599 (cond-mat/9710040). E. Brézin and A. Zee, *Nucl. Phys.* **B 509** (1998) 599 (cond-mat/9708029); C. Mudry, P. Brouwer, B. Halperin, V. Gurarie and A. Zee, *Phys. Rev.* **B 58** (1998) 13539.

P. W. Brouwer, *Phys. Rev.* **B 57** (1998) 10526 (cond-mat/9711113).

P. W. Brouwer, C. Mudry, B. D. Simons and A. Altland, *Phys. Rev. Lett.* **81** (1998) 862 (cond-mat/9807189).

C. Mudry, B. D. Simons and A. Altland, *Phys. Rev. Lett.* **80** (1998) 4257 (cond-mat/9712103).

R. A. Janik, M. A. Nowak, G. Papp and I. Zahed, *Acta. Phys. Polon.* **B 30** (1999) 45 (cond-mat/9705098).

I. Y. Goldsheid and B. A. Khoruzhenko, preprint cond-mat/9707230.

I. V. Yurkevich and I. V. Lerner, *Phys. Rev. Lett.* **82** (1999) 5080.

P. W. Brouwer, P. G. Silvestrov and C. W. J. Beenakker, *Phys. Rev.* **B 56** (1997) 4333 (cond-mat/9705186); P. G. Silvestrov, *Phys. Rev.* **B 58** (1998) 10111 (cond-mat/9802219); *Phys. Rev. Lett.* **82** (1999) 3140 (cond-mat/9804093); cond-mat/0008118.

L. N. Trefethen, M. Contedini and M. Embree, cond-mat/0003514 (submitted to SIAM J. Appl. Math).

B. Derrida, J. L. Jacobsen and R. Zeitak, *Jour. Stat. Phys.* **98** (2000) 31 (cond-mat/9906235)

G. M. Cicuta, M. Contedini and L. Molinari, cond-mat/9907014; L. Molinari, *J. Phys. A-Math. Gen.* **31** (1998) 8553.

J. Miller and Z. J. Wang, *Phys. Rev. Lett.* **76** (1996) 1461.

J. T. Chalker and Z. Jane Wang, *Phys. Rev. Lett.* **79** (1997) 1797, *Phys. Rev.* **E61** (2000) 196.

V.G.Benza, cond-mat/0006029; G.C.Ferrario and V.G.Benza *J. Phys. (Con-*

*dens. Matt.*) **11** (1999) 7557 (cond-mat/9907011).

A. V. Izyumov and B. D. Simons, *Phys. Rev. Lett.* **83** (1999) 4373 (cond-mat/9910163); *Europhys. Lett.* **45** (1999) 290 (cond-mat/9811260); A. V. Izyumov and K. V. Samokhin, *J. Phys. A-Math. Gen.* **32** (1999) 7843 (cond-mat/9909407).

B. Mehlig and J.T. Chalker, *Jour. Math. Phys.* **41** (2000) 3233 (cond-mat/9906279), *Phys. Rev. Lett.* **81** (1998) 3367 (cond-mat/9809090), *Ann. der Phys. (Berlin)* **7** (1998) 427.

R. A. Janik, W. Noerenberg, M. A. Nowak, G. Papp and I. Zahed, *Phys. Rev. E* **60** (1999) 2699 (cond-mat/9902314).

S. Hikami and R. Pnini, *J. Phys. A-Math. Gen.* **31** (1998) L587 (cond-mat/9806254).

A. Sedrakyan, *Nucl. Phys.* **B 554** (1999) 554 (cond-mat/9806301).

A.A. Andrianov, F. Cannata, J.P. Dedonder and M.V. Ioffe, *Int. J. Mod. Phys. A* **14** (1999) 2675 (quant-ph/9806019); F. Cannata, G. Junker and J. Trost *Phys. Lett. A* **246** (1998) 219 (quant-ph/9805085); X.-B. Wang, L. C. Kwek and C. H. Oh, *Phys. Lett. A* **259** (1999) 7.

[2] R. A. Janik, M. A. Nowak, G. Papp and I. Zahed, *Nucl. Phys.* **B 501** (1997) 603.

R. A. Janik, M. A. Nowak, G. Papp J. Wambach and I. Zahed, *Phys. Rev. E* **55** (1997) 4100.

[3] J. Feinberg and A. Zee, *Nucl. Phys.* **B 504** (1997) 579 (cond-mat/9703087).

[4] J. Feinberg and A. Zee, *Nucl. Phys.* **B 501** (1997) 643 (cond-mat/9704191).

[5] J. J. M. Verbaarschot and T. Wettig, Random Matrix Theory and Chiral Symmetry in QCD, hep-ph/0003017 (Submitted to Ann.Rev.Nucl.Part.Sci.)

D. Toublan and J. J. M. Verbaarschot, Effective Low-Energy Theories and QCD Dirac Spectra, hep-th/0001110

J. J. M. Verbaarschot, The Infrared Limit of the QCD Dirac Spectrum and Applications of Chiral Random Matrix Theory to QCD, hep-ph/9902394; Characterization of Universal Behavior in QCD Dirac Spectra, hep-th/9807070; Random Matrix Theory and QCD at Nonzero Chemical Potential, *Nucl. Phys. A* **642** (1998) 305. (hep-ph/9807296); Universal Behavior in Dirac Spectra, hep-th/9710114; Universal Fluctuations in Dirac Spectra, hep-th/9709032

R. A. Janik, M. A. Nowak, G. Papp and I. Zahed, Green's Functions in Nonhermitean Random Matrix Models, cond-mat/9909085; Various Shades of Blue's Functions, *Acta Phys. Polon. B* **28** (1997) 2949 (hep-th/9710103); Random Matrices and Chiral Symmetry in QCD, hep-ph/9806370; New Developments in Nonhermitean Random Matrix Models, hep-ph/9708418.

A. Zee, A Non-Hermitean Particle in a Disordered World, *Physica A* **254** (1998) 300 (cond-mat/9711114).

N. Hatano, Localization in Non-Hermitean Quantum Mechanics and Flux-Line Pinning in Superconductors, *Physica A* **254** (1998) 317 (cond-mat/9801283).

Y. V. Fyodorov, Almost-Hermitean Random Matrices: Applications to the Theory of Quantum Chaotic Scattering and Beyond, published in *Supersymmetry and Trace Formulas: Chaos and Disorder*, I. Lerner et al. (Editors), Kluwer Academic/Plenum Publishers, NY 1999, p. 293.

[6] E. Brézin, C. Itzykson, G. Parisi and J. -B. Zuber, *Comm. Math. Phys.* **59** (1978) 35.

[7] See for example, E. Brézin and A. Zee, *Phys. Rev. E* **49** (1994) 2588.

[8] E. Brézin and A. Zee, *Comp. Rend. Acad. Sci.*, (Paris) **317** (1993) 735.

[9] E. Brézin and J. Zinn-Justin, *Phys. Lett B* **288** (1992) 54.

S. Higuchi, C. Itoh, S. Nishigaki and N. Sakai, *Phys. Lett. B* **318** (1993) 63; *Nucl. Phys. B* **434** (1995) 283, Err.-ibid. **441** (1995) 405.

[10] J. D'Anna and A. Zee, *Phys. Rev. E* **53** (1996) 1399.

- [11] J. Feinberg and A. Zee, *Jour. Stat. Phys.* **87** (1997) 473 (cond-mat/9609190).
- [12] J. Ginibre, *Jour. Math. Phys.* **6** (1965) 440.
- [13] E.P. Wigner, Can. Math. Congr. Proc. p.174, University of Toronto Press (1957), reprinted in C. E. Porter, *Statistical Theories of Spectra: Fluctuation* (Academic, New York, 1965). See also M. L. Mehta, *Random Matrices* (Academic, New York, 1991).
- [14] A. Zee, *Nucl. Phys.* **B474** (1996) 726.  
See also P. Zinn-Justin, *Phys. Rev.* **E 59** (1999) 4884.
- [15] E. Brézin, S. Hikami and A. Zee, *Phys. Rev.* **E 51** (1995) 5442.
- [16] E. Brézin, S. Hikami and A. Zee, *Nucl. Phys.* **B 464** (1996) 411.
- [17] There are many papers on chiral matrices. A partial list which concentrates on Gaussian ensembles:  
J. J. M. Verbaarschot, *Nucl. Phys.* **B426** (1994) 559; J. J. M. Verbaarschot and I. Zahed, *Phys. Rev. Lett.* **70** (1993) 3852.  
K. Slevin and T. Nagao, *Phys. Rev. Lett.* **70** (1993) 635, *Phys. Rev.* **B 50** (1994) 2380; T. Nagao and K. Slevin, *J. Math.Phys.* **34** (1993) 2075, 2317.  
T. Nagao and P. J. Forrester, *Nucl. Phys.* **B 435** (FS) (1995) 401.  
A. V. Andreev, B. D. Simons and N. Taniguchi, *Nucl. Phys.* **B 432** (1994) 485.  
S. Hikami and A. Zee, *Nucl. Phys.* **B 446**, (1995) 337; S. Hikami, M. Shirai and F. Wegner, *Nucl. Phys.* **B 408** (1993) 415.  
C.B. Hanna, D.P. Arovas, K. Mullen and S.M. Girvin, cond-mat 9412102.
- [18] G.M. Cicuta and E. Montaldi, *Phys. Rev.* **D 29** (1984) 1267; A. Barbieri, G.M. Cicuta and E. Montaldi, *Nuov. Cim.* **84 A** (1984) 173; C.M. Canali, G.M. Cicuta, L. Molinari and E. Montaldi, *Nucl. Phys.* **B 265**, (1986) 485; G.M. Cicuta, L. Molinari, E. Montaldi and F. Riva, *J. Math.Phys.* **28** (1987) 1716.

- [19] J. Ambjørn, “Quantization of Geometry”, in Les Houches, Session LXII (1994), “Fluctuating Geometries in Statistical Mechanics and Field Theory”, edited by F. David, P. Ginsparg and J. Zinn-Justin (Elsevier 1996). See section 4.3 and references therein; J. Ambjørn, J. Jurkiewicz, and Yu. M. Makeenko, *Phys. Lett.* **B251** (1990) 517; S. Nishigaki *Phys. Lett.* **B 387** (1996) 139.
- [20] R. C. Myers and V. Periwal, *Nucl. Phys.* **B 390**, (1991) 716.  
A. Anderson, R. C. Myers and V. Periwal, *Phys. Lett.* **B 254** (1991) 89, *Nucl. Phys.* **B 360**, (1991) 463.
- [21] F. David, *Nucl. Phys.* **B 348**, (1991) 507.  
J. Jurkiewicz, *Phys. Lett.* **B 245** (1990) 178.  
For a more recent paper and more references on hermitean matrix models with multicut eigenvalue distribution see e.g. G. Akemann, *Nucl. Phys.* **B 482**, (1996) 403.

N=128

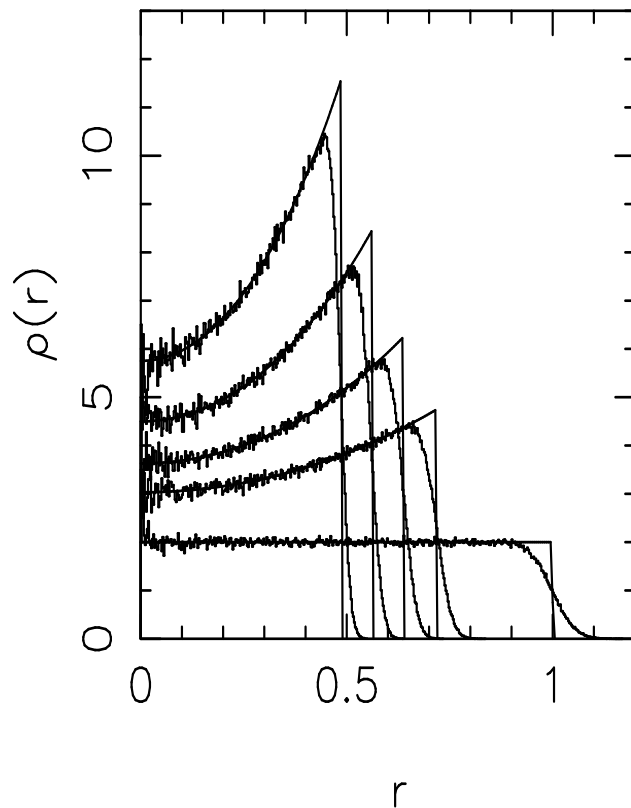


Figure 1: Comparison between Monte-Carlo measurements of the density of eigenvalues  $\rho(r)$  of matrices  $\phi$  of size  $128 \times 128$ , taken from the quartic ensemble  $V(\phi^\dagger\phi) = 2m^2\phi^\dagger\phi + g(\phi^\dagger\phi)^2$  with  $m^2 = 0.5$  (disk phase) and for  $g = 0, 0.5, 1, 2, 4$  ( $g$  increases from bottom to top), compared to the analytical results of [4] (solid lines). At  $g = 0$  we obtain Ginibre's Gaussian ensemble with  $V = \phi^\dagger\phi$ , with its unit disk of eigenvalues.

N=64,128,256

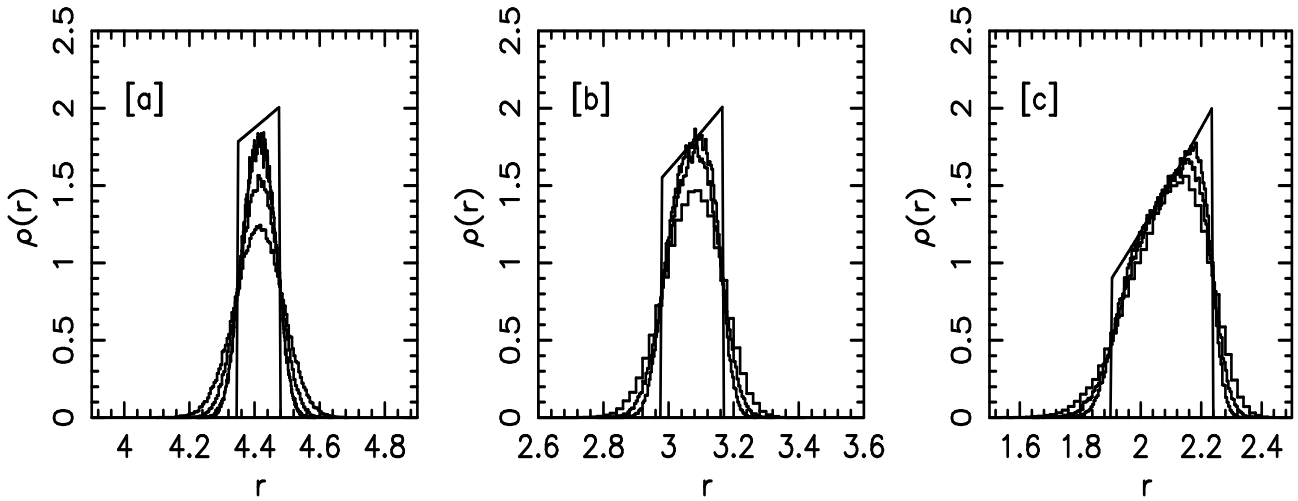


Figure 2: Results of Monte-Carlo measurements of the density of eigenvalues  $\rho(r)$  of matrices  $\phi$  of sizes corresponding to  $N = 64, 128$  and  $256$ , taken from the quartic ensemble with  $m^2 = -\mu^2 = -0.5$  (annular phase) for various values of the quartic coupling:  $g = 0.025$  in [a],  $g = 0.05$  in [b] and  $g = 0.1$  in [c]. These are compared to the analytical results of [4] (solid lines). As  $N$  increases, the numerical results converge monotonically to the analytical results.

N=128

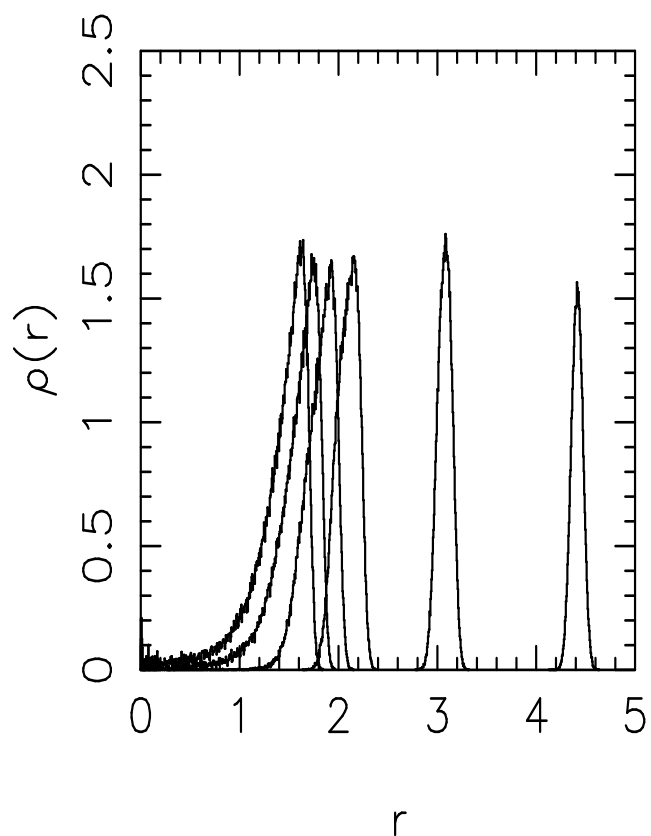


Figure 3: Monte-Carlo measurements of the density of eigenvalues  $\rho(r)$  of matrices  $\phi$  of size 128x128, taken from the the quartic ensemble with  $\mu^2 = 0.5$  and for  $g = 0.025, 0.05, 0.1, 0.125, 0.15$  and  $0.175$  ( $g$  increases from right to left). The first three profiles on the right (corresponding to the three lowest values of  $g$ ) evidently belong to the annular phase. The fourth density profile from the right is the critical one (corresponding to  $g_c = 0.125$ ). Finally, The last two profiles (which correspond to the two higher values of  $g$ ) belong to the disk configuration.

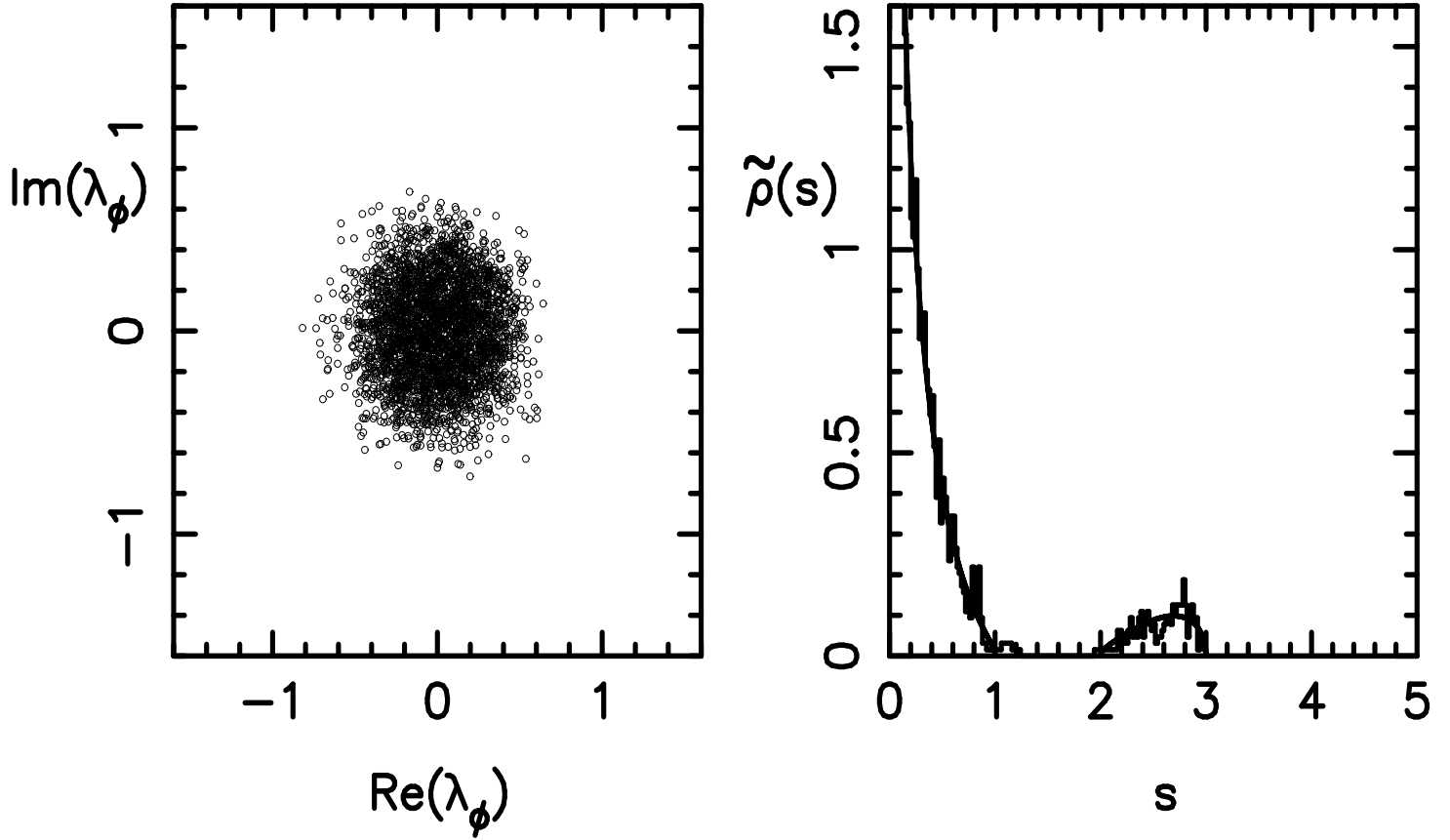


Figure 4: Scatter plot of the eigenvalues of matrices  $\phi$  of size  $32 \times 32$ , taken from (5.1) with  $m^2 = 7.372$ ,  $\lambda = -6.116$  and  $g = 1.372$  (left), and the corresponding density of eigenvalues  $\tilde{\rho}(s)$  of  $\phi^\dagger \phi$  (right). The solid line on the right is the analytical curve corresponding to (A.22). The support of  $\tilde{\rho}(s)$  is split into the two segments  $\{0 \leq s \leq a = 1\} \cup \{b = 2 \leq s \leq c = 3\}$ , while the support of  $\rho(r)$  on the left is manifestly a disk.

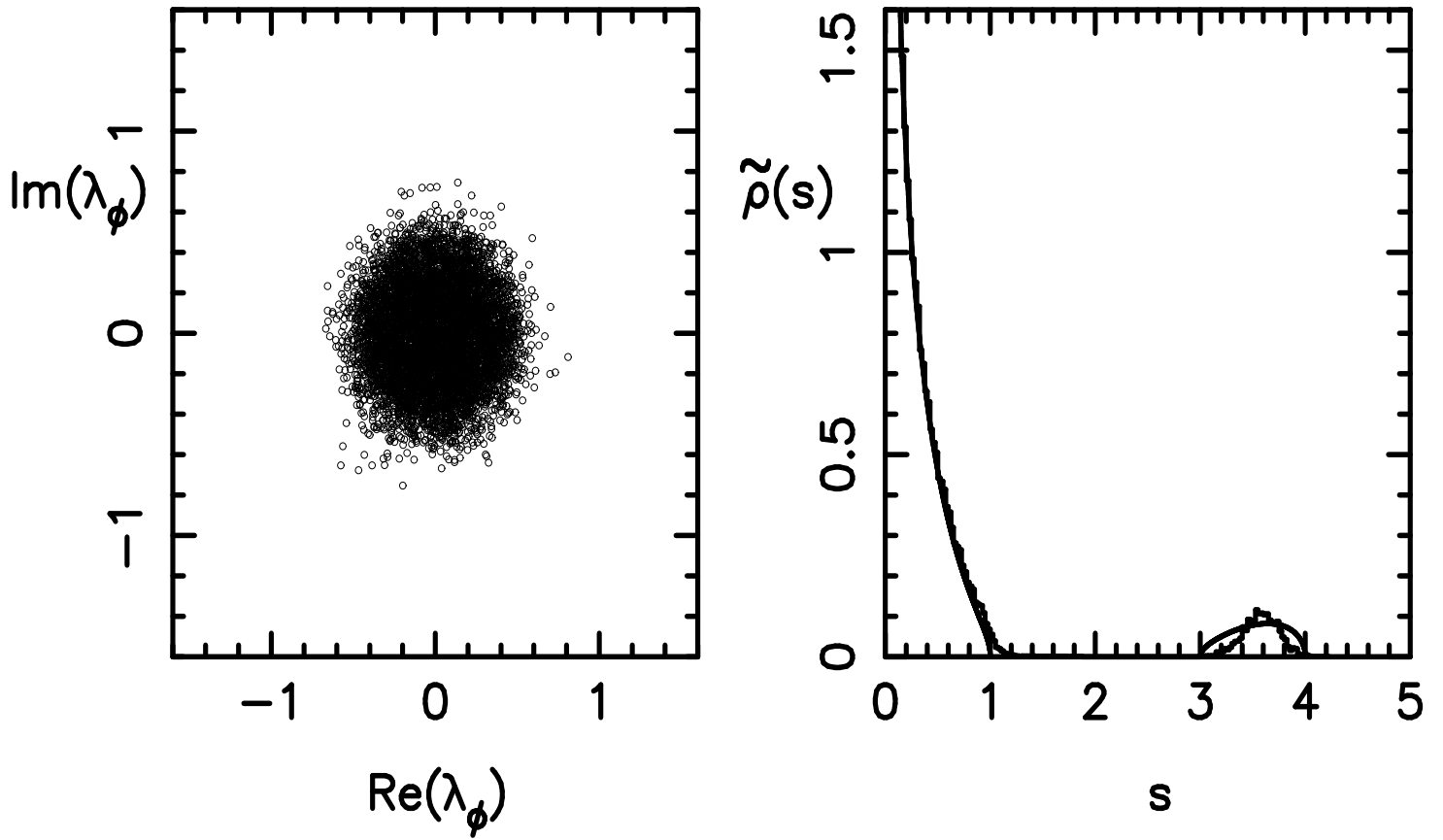


Figure 5: Similarly to Figure 4, but with  $m^2 = 6.403$ ,  $\lambda = 4.184$  and  $g = 0.713$ . The support of  $\tilde{\rho}(s)$  is split into the two segments  $\{0 \leq s \leq a = 1\} \cup \{b = 3 \leq s \leq c = 4\}$ , while the support of  $\rho(r)$  on the left remains a disk.